Analytica Chimica Acta 792 (2013) 101–109

Contents lists available at SciVerse ScienceDirect

Analytica Chimica Acta

journal homepage: www.elsevier.com/locate/aca

A colloidal suspension of nanostructured poly(*N*-butyl benzimidazole)-graphene sheets with high oxidase yield for analytical glucose and choline detections

Hsiao-Chien Chen[a,b,c], Rung-Ywan Tsai[d], Yen-Hsuan Chen[a], Ren-Shen Lee[e], Mu-Yi Hua[a,b,c,*]

[a] Department of Chemical and Materials Engineering, Chang Gung University, Tao-Yuan 33302, Taiwan, ROC
[b] Biomedical Engineering Research Center, Chang Gung University, Tao-Yuan 33302, Taiwan, ROC
[c] Green Technology Research Center, Chang Gung University, Tao-Yuan 33302, Taiwan, ROC
[d] Electronics and Optoelectronics Research Laboratories, Industrial Technology Research Institute, Hsinchu 31040, Taiwan, ROC
[e] Center of General Education, Chang Gung University, Tao-Yuan 33302, Taiwan, ROC

HIGHLIGHTS

- A high stability, selectivity, and sensitivity biosensor for glucose detection.
- This sensor has intrinsic hydrogen peroxide catalytic activity.
- A non-destructive immobilization is used to preserve high enzyme bioactivity.
- A favorable platform for the development of oxidase-based biosensors.

GRAPHICAL ABSTRACT

(A) The mechanism of glucose detection by the GOD-PBBIns-Gs/Au electrode. (B) A diagram depicting the preparation of the GOD-PBBIns-Gs/Au electrode. (C) Photographs of PBBIns-Gs (left), GOD (middle), and PBBIns-Gs mixed with GOD (right) in DI water over time.

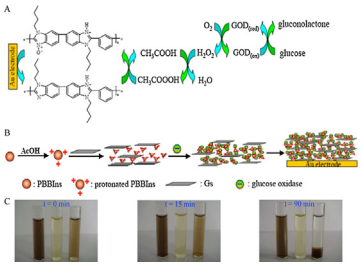

ARTICLE INFO

Article history:
Received 5 January 2013
Received in revised form 17 June 2013
Accepted 3 July 2013
Available online 9 July 2013

Keywords:
Poly(*N*-butyl benzimidazole)
Graphene sheet
Hydrogen peroxide
Glucose
Choline
Electrostatic attraction

ABSTRACT

A colloidal suspension of nanostructured poly(*N*-butyl benzimidazole)-graphene sheets (PBBIns-Gs) was used to modify a gold electrode to form a three-dimensional PBBIns-Gs/Au electrode that was sensitive to hydrogen peroxide (H_2O_2) in the presence of acetic acid (AcOH). The positively charged nanostructured poly(*N*-butyl benzimidazole) (PBBIns) separated the graphene sheets (Gs) and kept them suspended in an aqueous solution. Additionally, graphene sheets (Gs) formed "diaphragms" that intercalated Gs, which separated PBBIns to prevent tight packing and enhanced the surface area. The PBBIns-Gs/Au electrode exhibited superior sensitivity toward H_2O_2 relative to the PBBIns-modified Au (PBBIns/Au) electrode. Furthermore, a high yield of glucose oxidase (GOD) on the PBBIns-Gs of 52.3 mg GOD per 1 mg PBBIns-Gs was obtained from the electrostatic attraction between the positively charged PBBIns-Gs and negatively charged GOD. The non-destructive immobilization of GOD on the surface of the PBBIns-Gs (GOD-PBBIns-Gs) retained 91.5% and 39.2% of bioactivity, respectively, relative to free GOD for the colloidal suspension of the GOD-PBBIns-Gs and its modified Au (GOD-PBBIns-Gs/Au) electrode. Based on advantages including a negative working potential, high sensitivity toward H_2O_2, and non-destructive immobilization, the proposed glucose biosensor based on an GOD-PBBIns-Gs/Au electrode exhibited a fast response time (5.6 s), broad detection range (10 μM to 10 mM), high sensitivity (143.5 $\mu A\,mM^{-1}\,cm^{-2}$) and selectivity, and excellent stability. Finally, a choline biosensor was developed by dipping a PBBIns-Gs/Au electrode

* Corresponding author at: Department of Chemical and Materials Engineering, Chang Gung University, Tao-Yuan 33302, Taiwan, ROC. Tel.: +886 3 2118800x5289; fax: +886 3 2118668.
E-mail address: huamy@mail.cgu.edu.tw (M.-Y. Hua).

0003-2670/$ – see front matter
http://dx.doi.org/10.1016/j.aca.2013.07.006

into a choline oxidase (ChOx) solution for enzyme loading. The choline biosensor had a linear range of 0.1 μM to 0.83 mM, sensitivity of 494.9 μA mM^{-1} cm^{-2}, and detection limit of 0.02 μM. The results of glucose and choline measurement indicate that the PBBIns-Gs/Au electrode provides a useful platform for the development of oxidase-based biosensors.

1. Introduction

Diabetic patients are at increased risk for developing retinopathy, nephropathy, and other complications that directly relate to blood glucose concentration [1]. Therefore, the development of a glucose biosensor for clinical application is critical. Biosensors based on electrochemical technology have received increasing attention because they are simple to use and highly sensitive for real-time detection [2,3]. Glucose oxidase (GOD) has been widely used for the fabrication of enzymatic electrodes [4,5]. Because GOD can oxidize glucose to gluconolactone and H_2O_2 in the presence of oxygen, glucose measurement has been based on the detection of released H_2O_2 or consumed oxygen using electrochemical techniques [6,7]. The most commonly used method based on H_2O_2 detection is direct electrocatalysis at working potentials of 0.5–0.7 V [8,9]. However, the high over-potential required generates a response that interferes with quantification of the analyte [10]. Use of the high selectivity of polyphenylenediamine film with an anti-interference characteristic may be a potential strategy [11], but this approach usually decreases the reproducibility and sensitivity of the biosensor [12,13]. Recently, many studies have focused on working at a relatively lower potential to prevent this interference with techniques including electrochemical deposition of a dense redox-active Prussian blue (PB) layer or immobilization of bienzymes (oxidase and peroxidase) simultaneously [14–18]. However, biosensors based on bienzymes require two expensive enzymes and issues arise related to competition between the enzymes.

Additionally, biosensor performance is mainly affected by the enzyme immobilization. Mediators used for enzyme immobilization can improve stability under extreme conditions and are quite useful for biosensors. Many researchers have attempted to immobilize enzymes by methods including electrostatic interaction with polyelectrolyte [19,20], entrapment [21,22], electrodeposition [23], mixing in a carbon composite [24,25], layer-by-layer assembly [26–28], and covalent bonding [29,30]. The electrostatic technique is widely recognized as an ideal candidate because the bioactivity of the immobilized enzyme is well preserved. Several studies have focused on modifying the substrate surface using plasma or by mixing with poly(diallyldimethylammonium chloride) to transfer the electrostatic charge of the substrate materials to a positive charge [31,32]. This state provides a favorable condition to adsorb negatively charged GOD and improves biosensor fabrication.

Currently, most glucose biosensors based on a polymer-modified electrode are developed by direct electrocatalysis of H_2O_2 because peroxidase is not present [33,34]. In our previous study, we found that synthesized poly(*N*-butyl benzimidazole) (PBBI) was sensitive to H_2O_2 in the presence of acetic acid (AcOH) and generated a response current at negative potentials. The proposed H_2O_2 sensor exhibited high selectivity and thermal stability. After modification, the nanostructured PBBI (PBBIns) was dispersed and well suspended in aqueous solution, which greatly enhanced sensitivity [35]. However, the proton that dissociates from acetic acid would occupy the electroactive imine site and decrease sensitivity. This shortcoming was employed for adsorbing GOD by the electrostatic method to fabricate a glucose biosensor that utilizes the positively charged protonated imine. Moreover, the incorporated graphene sheets (Gs) were stably suspended within the PBBIns in aqueous solution and not packing tightly with each other during the drying process, which greatly increased the surface area.

2. Experimental

2.1. Chemicals

Isophthaloyl dichloride (98%) was from Acros. 3,3′-diaminobenzidine tetrahydrochloride hydrate (>97%), glucose oxidase (GOD, EC 232-601-0) from *Aspergillus niger* with an activity of 151 U mg^{-1}, and choline oxidase (ChOx) from *Alcaligenes* with an activity of 13 U mg^{-1} were from Sigma. Polyphosphoric acid, glucose, choline, and H_2O_2 (30 wt%) were from Showa. Dimethyl sulfoxide (DMSO) was from Tedia. Graphene was purchased from Strem Chemicals. The hydrogen peroxide assay kit was from BioVision. Sodium hydride was from Fluka and AcOH (99.8%) was from Scharlau. Deionized (DI) water was used in all experiments.

2.2. Instrumentation and measurements

Field-emission scanning electron microscopy (FE-SEM) was performed using a Hitachi S-5000 system. Absorption spectra were recorded on a PerkinElmer Lambda 800/900 spectrometer. X-ray diffraction (XRD) patterns were analyzed on a Rigaku D/Max-2B with nickel-filtered Cu Kα radiation at a scanning rate of 2°/min from 5° to 70°. Isoelectric point (IEP) and particle size were analyzed using a Malvern Zetasizer Nano ZS zeta potential analyzer. Electrochemical measurements were performed on a CHI 660A electrochemical workstation (CH Instruments, USA) with a three-electrode system consisting of the modified electrode, a bare Au electrode, and an Ag/AgCl electrode as the working, counter, and reference electrodes, respectively. All electrochemical measurements were performed in 40 mL of 0.2 M phosphate-buffered saline (PBS, pH 6.4) at 25 °C.

2.3. Procedures

2.3.1. Preparation of PBBIns and a colloidal suspension of PBBIns-Gs

The synthesis of PBBI and preparation of PBBIns have been previously reported [35]. Briefly, 0.23 g of PBBI dissolved in 10 mL of DMSO was dropped into a stirring poor solvent consisting of 250 mL of DI water and 150 mL of acetone. After high-speed centrifugation (5500 rpm), the nanoscale precipitate was dispersed into 10 mL of DI water. The preparation of a colloidal suspension of PBBIns-Gs was performed as follows: in addition to the above steps, acetic acid was added to the nanostructure PBBI solution to adjust the pH from 7.0 to 6.4. After high-speed centrifugation (5500 rpm), the nanoscale precipitate was washed with 20 mL of DI water and precipitated again by high-speed centrifugation. After this procedure was repeated three times, the acid-treated PBBIns were dispersed into 10 mL of DI water followed by the addition of 2.3 mg of Gs.

2.3.2. Preparation of PBBIns/Au and PBBIns-Gs/Au electrodes

Two microliters of the dispersed PBBIns and PBBIns-Gs solutions were dropped onto Au disk electrodes (0.196 cm^2) and dried in a vacuum aspirator at 50 °C for 5 h.

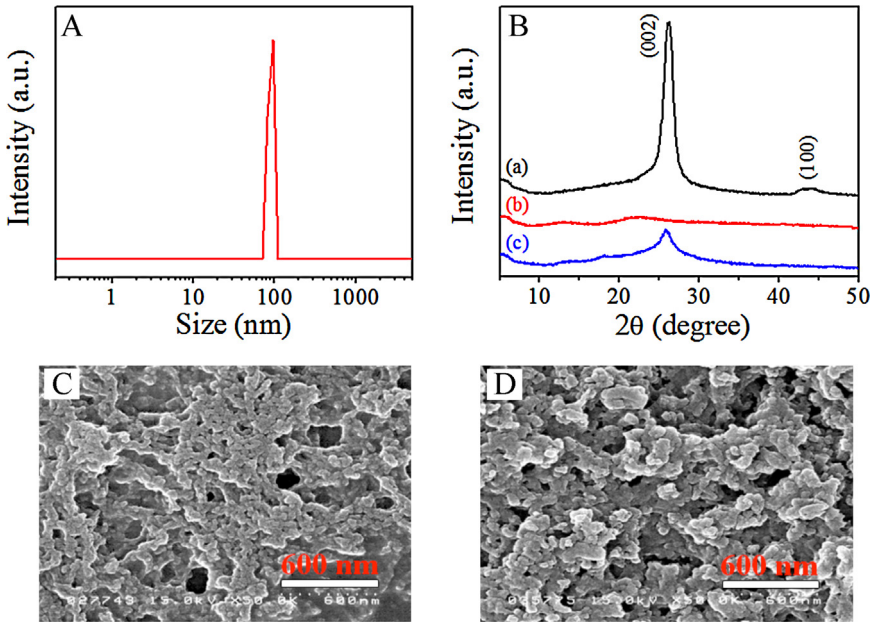

Fig. 1. (A) Particle size spectrum of PBBIns. (B) XRD patterns of (a) Gs, (b) PBBIns, and (c) PBBIns-Gs. Scanning electron micrographs of (C) PBBIns/Au and (D) PBBIns-Gs/Au electrodes.

2.3.3. Preparation of GOD-PBBIns/Au and GOD-PBBIns-Gs/Au electrodes

To prepare the GOD-PBBIns/Au and GOD-PBBIns-Gs/Au electrodes, 50 (L each of the PBBIns and PBBIns-Gs solutions was mixed with 10 mL of GOD solution (10 mg mL^{-1}) and incubated at 4 °C for 90 min. The two precipitates were washed with DI water three times and re-dispersed in 50 μL of DI water. Next, 2 μL of each solution was dropped onto the respective Au electrode surfaces and dried at 4 °C for 2 h before measurement.

2.3.4. GOD bioactivity assay of GOD-PBBIns and GOD-PBBIns-Gs

The bioactivity assay was based on the concentration of released H_2O_2 after reaction with 5 mL of glucose (2 mM) for 1 min under saturated oxygen in PBS (pH 6.4). The quantification of H_2O_2 was performed using a H_2O_2 assay kit, and H_2O_2 was detected by measuring the absorbance at 570 nm.

3. Results and discussion

3.1. Characteristics of PBBIns and PBBIns-Gs

The size distribution of synthesized PBBIns was analyzed by a particle size analyzer and is presented in Fig. 1A. The sharp peak indicates a uniform particle size of 90 nm in DI water. However, the particle shape was not observed in the SEM image (Fig. 1C). The PBBIns were likely formed without a stiff core to maintain their shape and deformed to a slightly planiform structure during the drying process. In addition, the heavy packing led to a flatter inner bottom, which could be improved by the incorporation of Gs that would intercalate and separate PBBIns to form a colloidal suspension of PBBIns-Gs. Moreover, the acid-treated PBBIns with a positive charge improved Gs suspension and did not precipitate in DI water. This phenomenon was similar to reports that polyelectrolytes could facilitate carbon nanotube or Gs suspension in aqueous solution [36,37]. The intercalation was demonstrated by an XRD pattern (Fig. 1B). The diffraction peaks of Gs at $2\theta = 26.2°$ and 43.5° were attributed to the graphite-like structure (0 0 2) and (1 0 0), respectively [Fig. 1B(a)] [38]. A broad characteristic peak of amorphous PBBIns appeared at approximately $2\theta = 22°$ [Fig. 1B(b)]. After mixing, the sharp Gs peak at 26.2° decreased and shifted to 25.7°, and the peak at 43.5° disappeared, which implies that the PBBIns served as placeholders to prevent individual Gs from re-stacking during the drying process. Therefore, Gs acted as "diaphragms" to prevent tight packing of the PBBIns. The SEM image of PBBIns-Gs is presented in Fig. 1D. The "constructed diaphragm" not only displayed a more three-dimensional surface than PBBIns but also generated more channels to the inner layers.

3.2. Electrochemical behavior of the PBBIns-Gs/Au electrode

Cyclic voltammograms (CV) of the Gs/Au, PBBIns/Au, and PBBIns-Gs/Au electrodes were recorded in 0.2 M PBS at pH 6.4 (Fig. 2A). No redox peaks were observed from the Gs/Au electrode [Fig. 2A(a)]. However, the PBBIns/Au electrode exhibited one pair of redox peaks at 0.11 V for the oxidative peak and −0.08 V for the reductive peak with a peak-to-peak separation (ΔE) of 0.19 V [Fig. 2A(b)]. These two peaks were attributed to the electrochemical behavior of an electroactive imine [39,40]. Moreover, after the addition of Gs, the PBBIns-Gs/Au electrode exhibited a pair of redox peaks at 0.13 V for the oxidative peak and −0.03 V for the reductive peak with a ΔE of 0.16 V [Fig. 2A(c)]. The smaller ΔE indicated that the electrochemical behavior became more reversible because of the enhancement of electron transfer by Gs [36,41]. To further understand the kinetics of this electron transfer process, the effects of varying the scan rate (() on the peak currents of the PBBIns-Gs/Au electrode were evaluated. The peak current increased concomitantly with (from 0.05 to 0.5 V s^{-1} (Fig. 2B). Furthermore, the peak currents of the electroactive imines were proportional to the square root of the ((Fig. 2C), which was a characteristic of the diffusion-controlled process [40,42]. Additionally, the reduction and oxidation peak potentials shifted negatively and positively as (increased. At high scan rates, the surface electrochemical reaction became irreversible, and the peak potentials were proportional to the natural logarithm of (: they were $E_{pa} = 0.256 + 0.0583 \ln($ for the oxidation potential and $E_{pc} = -0.137 - 0.0504 \ln($ for the reduction potential (Fig. 2D). According to Laviron's equations [43,44]:

$$\alpha = \frac{k_a}{(k_a - k_c)} \quad (1)$$

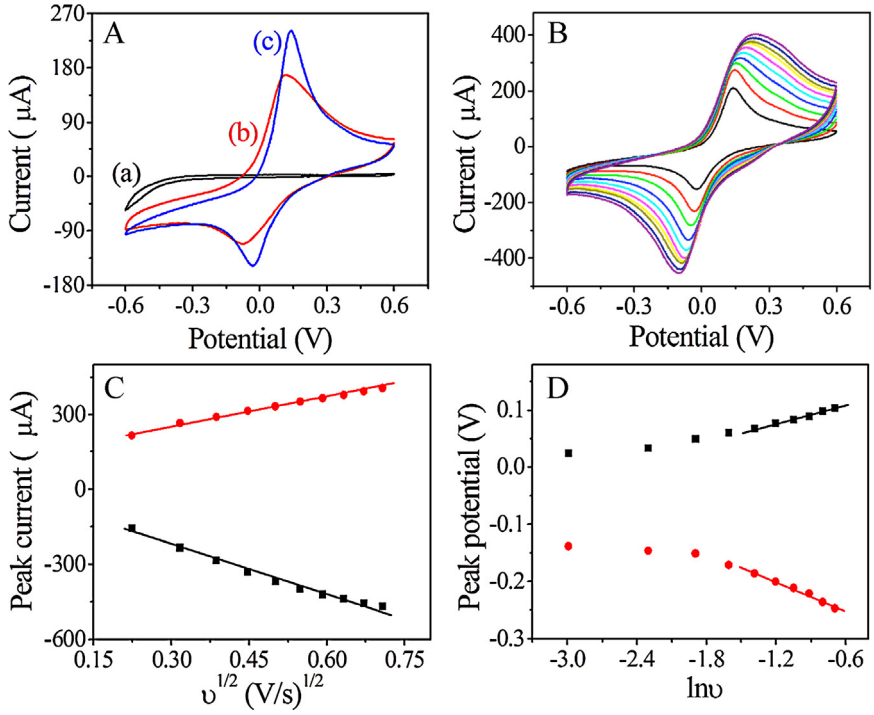

Fig. 2. (A) CVs of (a) Gs/Au, (b) PBBIns/Au, and (c) PBBIns-Gs/Au electrodes. (B) CVs of PBBIns-Gs/Au electrode at scan rates ranging from 0.05 to 0.5 V s^{-1}. (C) Linear relationship of peak current vs. $\upsilon^{1/2}$ for the PBBIns-Gs/Au electrode. (D) Linear relationship of peak potential vs. ln υ for the PBBIns-Gs/Au electrode (these experiments were performed at pH 6.4 with under saturated nitrogen).

$$E_{pa} = E^{0'} - \frac{RT}{(1-\alpha)nF} \ln \frac{RTk_s}{(1-\alpha)nF} + \frac{RT}{(1-\alpha)nF} \ln \upsilon \quad (2)$$

$$E_{pc} = E^{0'} + \frac{RT}{\alpha nF} \ln \frac{RTk_s}{\alpha nF} - \frac{RT}{\alpha nF} \ln \upsilon \quad (3)$$

where (is the electron transfer coefficient, k_a and k_c are the slopes of E_{pa} and E_{pc} versus ln (, n is the electron transfer number, k_s is the electron transfer rate constant, F is Faraday's constant, and $E^{0'}$ is the formal potential (i.e., $[E_{pa} + E_{pc}]/2$), the estimated α and n values were 0.54 and 0.95, respectively. The electron transfer number, n, was approximately 1.0 and was in accordance with the electrochemical behavior of the imine structure documented in the literature. Furthermore, the calculated k_s of the PBBIns-Gs/Au electrode was 0.57 s^{-1}, which was greater than the value of 0.36 s^{-1} obtained for the PBBIns/Au electrode and thus demonstrates that Gs enhanced the electron transfer and improved the reversibility of reducing the ΔE. According to Faraday's law, $Q = nFA\Gamma$ (where Q is the charge from the anodic peak and A is the surface area of the electrode), the surface concentration (Γ) of the electroactive imine was approximately 1.45×10^{-8} mol cm^{-2}, which was greater than the value of 9.68×10^{-9} mol cm^{-2} observed for the PBBIns/Au electrode and thus indicates that the Gs could generate "diaphragms" to prevent tight packing of the PBBIns. These "diaphragms" created channels that allowed PBS to diffuse freely to the inner layers and increased the surface area.

3.3. PBBIns-Gs/Au electrode-based H_2O_2 biosensor

Previously, it was demonstrated that the imine structure was sensitive to H_2O_2 in the presence of AcOH to form *N*-oxide [35]. In addition, this oxide could be reversed electrochemically to generate a current response. Based on this mechanism, the H_2O_2 sensor was developed. The PBBIns-Gs/Au electrode was also tested by CV performed at pH 6.4 in PBS, which is presented in Fig. 3A. The reduction current increased and the oxidation current decreased when 1 mM H_2O_2 was added [Fig. 3A(b)]. At a potential of −0.5 V, the current increased to 33.2 μA, which was greater than the value of 23.4 μA observed for the PBBIns/Au electrode (Fig. 3A(e) inset). Furthermore, this phenomenon was more pronounced as the H_2O_2 concentration was increased to 2 mM [Fig. 3A(c)]. These data imply that the PBBIns-Gs/Au electrode is highly sensitive to H_2O_2.

Therefore, the performance of the H_2O_2 sensor based on a PBBIns-Gs/Au electrode was studied by injecting it with different H_2O_2 concentrations. Fig. 3B depicts the amperometric responses of the modified electrode during successive addition of H_2O_2 into a continuously stirred PBS solution (stirring rate 400 rpm, pH 6.4) at an applied potential of −0.5 V. The sensor displayed a rapid and sensitive response to H_2O_2 and achieved 95% of the steady-state current within 4.7 s, which indicates that the PBBIns-Gs/Au electrode had good electrocatalytic reduction and fast electron exchange behavior. The response to H_2O_2 was linear from 6.25 μM to 15.0 mM with a sensitivity of 855.8 μA mM^{-1} cm^{-2} (Fig. 3C). The detection limit was estimated to be 2.3 μM with a signal-to-noise ratio of 3 ($S\,N^{-1} = 3$). The sensor's performance was better than that of the PBBIns/Au electrode, most likely because of the increased electron transfer and surface area provided by Gs. In addition, the highly sensitive PBBIns-Gs/Au electrode-based H_2O_2 sensor has potential in the development of a glucose biosensor.

3.4. GOD immobilization and bioactivity assay

The PBBIns-Gs/Au electrode offers amperometric potential for the analytical detection of H_2O_2. This electrode could be used to fabricate a glucose biosensor that utilizes the detection mechanism presented in Fig. 4A because H_2O_2 would be released during the reaction of glucose with glucose oxidase. Although the detection process was performed in the presence of AcOH, which would also occupy a proportion of the imine sites and decrease sensor performance, the positively charged protonated imine ($-\overset{+}{\underset{H}{N}}=$) was suitable for the immobilization of GOD by electrostatic attraction

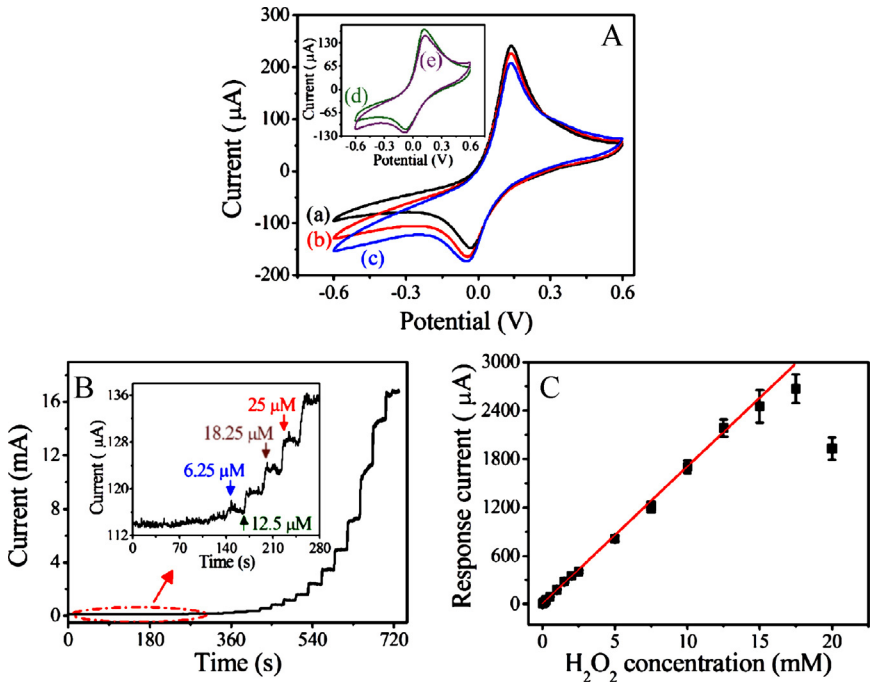

Fig. 3. (A) CVs of the PBBIns-Gs/Au electrode in the (a) absence and presence of (b) 1 mM and (c) 2 mM H_2O_2. Inset: CVs of the PBBIns/Au electrode in the (d) absence and (e) presence of 1 mM H_2O_2. (B) Current–time plot of the PBBIns-Gs/Au electrode after successive addition of H_2O_2 at increasing concentrations. (C) Linear dependence of the response currents on H_2O_2 concentration ($n = 5$).

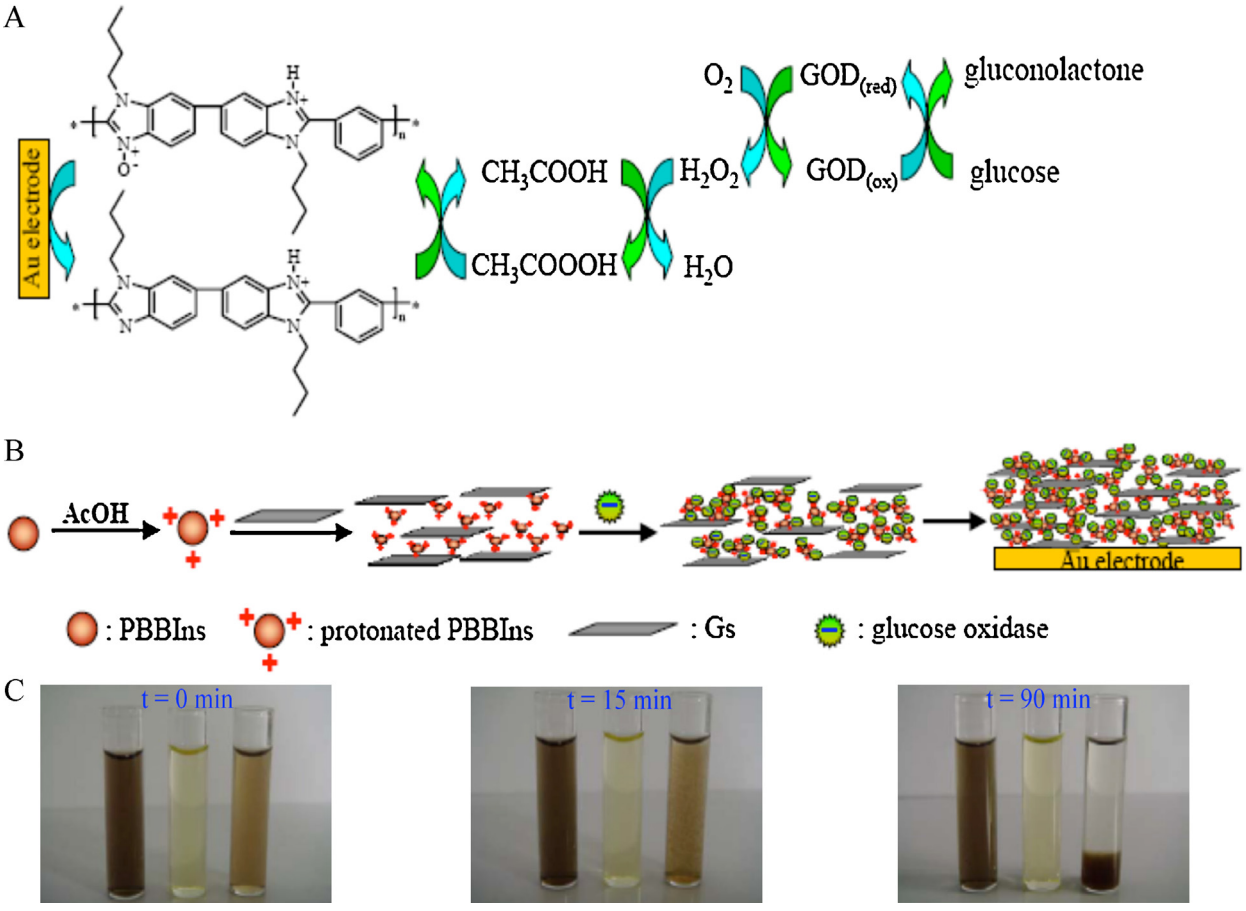

Fig. 4. (A) The mechanism of glucose detection by the GOD-PBBIns-Gs/Au electrode. (B) A diagram depicting the preparation of the GOD-PBBIns-Gs/Au electrode. (C) Photographs of PBBIns-Gs (left), GOD (middle), and PBBIns-Gs mixed with GOD (right) in DI water over time.

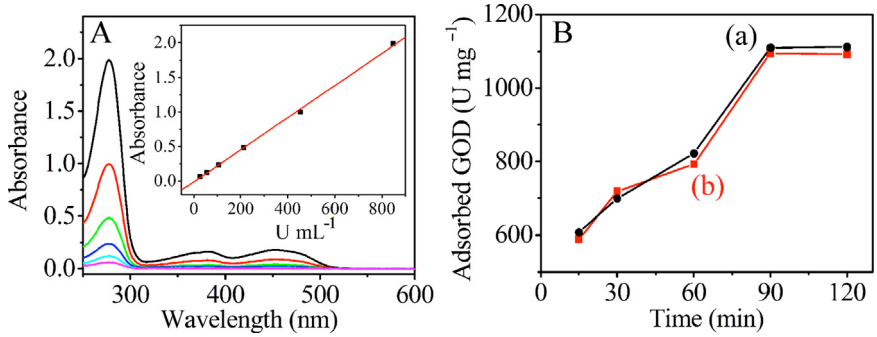

Fig. 5. (A) Absorption spectra of different GOD concentrations in DI water (inset: linear dependence of absorption intensity vs. bioactivity units at 277 nm). (B) The quantity of immobilized GOD in the colloidal suspensions of (a) PBBIns-Gs and (b) PBBIns.

(Fig. 4B). The isoelectric point (IEP) results indicate that the PBBIns-Gs charge converted from a positive charge (38.1 mV) to a highly negative charge (−17.5 mV), which demonstrates that sufficient GOD enzymes were attracted and immobilized on the PBBIns-Gs surface to successfully form the GOD-PBBIns-Gs complex. This phenomenon is clearly depicted in the photographs presented in Fig. 4C. The colloidal PBBIns-Gs could be suspended in DI water because of the acid-treated PBBIns-Gs that provided a positive charge from the protonated imine [Fig. 4C(a)]. Additionally, GOD was soluble in DI water and exhibited a yellow color. After mixing with GOD for 15 min, some species in solution had the appearance of cotton wool [Fig. 4C(b)]. Furthermore, these species precipitated at the bottom after 90 min and the solution was nearly colorless, which indicates that GOD was captured by PBBIns and served as a linkage within the PBBIns-Gs complex [Fig. 4C(c)].

In developing a glucose biosensor, the quantity and bioactivity of immobilized GOD are important factors for biosensor performance. To investigate the loading quantity of GOD, the absorption spectra of GOD in DI water were analyzed and are presented in Fig. 5A. A clear absorption peak was observed at 277 nm, and its intensity was proportional to the quantity of GOD. Therefore, the loading quantity of GOD on the PBBIns-Gs electrode could be estimated from the GOD remaining in the DI water. The loading quantity increased with time and was highest at 90 min, after which it equilibrated (Fig. 5B). The amount of GOD adsorbed was 1109.7 U (52.3 mg) per mg of PBBIns-Gs and was almost the same as the amount of PBBIns adsorbed (51.6 mg of GOD per mg of PBBIns), which indicates that Gs did not affect the electrostatic adsorption. The loading capacity was significantly higher than that for wet anion exchange resin (1.05 mg g^{-1}) because of the strong electrostatic attraction and nanostructure of PBBIns-Gs [45]. Furthermore, the immobilization technique preserved the bioactivity of GOD as expected. A hydrogen peroxide assay kit was used to assay the H_2O_2 concentration at a wavelength of 570 nm. After GOD-PBBIns-Gs was injected into 5 mL of 2 mM glucose under saturated oxygen for 1 min, the amount of released H_2O_2 was measured and compared to the amount of free GOD. The immobilized GOD maintained 91.5% relative bioactivity, which indicates that electrostatic adsorption did not destroy or inactivate the enzyme. After the colloid suspension of GOD-PBBIns-Gs was deposited on the Au electrode surface and dried at 4 °C for 2 h to prepare the GOD-PBBIns-Gs/Au electrode, the free and immobilized enzymes retained 39.2% and 42.8% bioactivity, respectively. After rinsing with DI water for 30 s, no absorption peak was observed at 277 nm, which indicates that the electrostatic interaction between the PBBIns-Gs and GOD was strong and stable. Therefore, the bioactivity of GOD from the GOD-PBBIns-Gs/Au electrode was calculated at 20 U, which was higher than the value of 10.7 U observed for the GOD-PBBIns/Au electrode. This result confirms the generation of "diaphragms" within the Gs that permit diffusion of glucose to the inner layers for reaction with GOD in the absence of electronic influence from Gs.

3.5. GOD-PBBIns-Gs/Au electrode-based glucose biosensor

Similar to the H_2O_2 detection methods, the electrochemical behavior of the GOD-PBBIns-Gs/Au electrode was studied by CVs at pH 6.4 under saturated oxygen (Fig. 6A). In the presence of 5 mM glucose, the reduction peak current increased as the oxidation peak current decreased; the electrochemical behavior was consistent with that of the PBBIns-Gs/Au electrode in H_2O_2 solution, which suggests that the glucose detection is feasible. Fig. 6B depicts the current-time curve for the successive addition of glucose at pH 6.4. To prevent possible interference from oxygen, a working potential of −0.3 V was chosen for glucose determination. In contrast to the currents observed for the GOD-PBBIns/Au electrode [Fig. 6B(b)], large stepwise currents were observed for the GOD-PBBIns-Gs/Au electrode [Fig. 6B(a)], which demonstrates that the GOD immobilized on the PBBIns-Gs had strong catalytic activity toward glucose. In contrast, no signal was observed based on the PBBI-Gs/Au electrode, meaning that glucose could not be catalyzed in the absence of GOD. The time required to reach a 95% response was less than 5.6 s. The corresponding calibration curve for glucose was linear from 10 μM to 10 mM with a relatively high sensitivity of 143.5 μA mM^{-1} cm^{-2} (Fig. 6B, inset). The uniform response time for each stepwise current and the linear dependence on glucose concentration demonstrate that the immobilized GOD was stable and did not detach from the PBBIns-Gs during detection. Moreover, relative to the GOD-PBBIns/Au electrode (Table 1), the glucose biosensor based on the GOD-PBBIns-Gs/Au electrode exhibited high performance with regard to sensitivity, detection range, and response time because of the increased surface area and electron transfer provided by Gs. The apparent Michaelis–Menten constant (K_m^{app}) for the GOD-substrate kinetics of the glucose-detecting GOD-PBBIns-Gs/Au electrode can be obtained from the Lineweaver–Burk equation [46]:

$$\frac{1}{I_{SS}} = \left(\frac{K_m^{app}}{I_{max}}\right)\left(\frac{1}{C}\right) + \frac{1}{I_{max}} \quad (4)$$

The K_m^{app} value for the GOD-PBBIns-Gs/Au electrode estimated from Fig. 6C was 0.54 mM, which was lower than that obtained in the covalent bonding (GOD/BSA/GNPs-Pb NWs/Pt electrode, 4.85 mM) and entrapped (Ti/NPAu/PB/GOx, 2.1 mM) enzyme immobilization methods [21,47]. The lower value indicates that GOD immobilized on the PBBIns-Gs/Au electrode retained its bioactivity and exhibited high biological affinity toward glucose, which was attributed to the non-destructive immobilization and electrostatic attraction. Relative to previous glucose biosensor reports, the GOD-PBBIns-Gs/Au electrode exhibited better sensitivity and

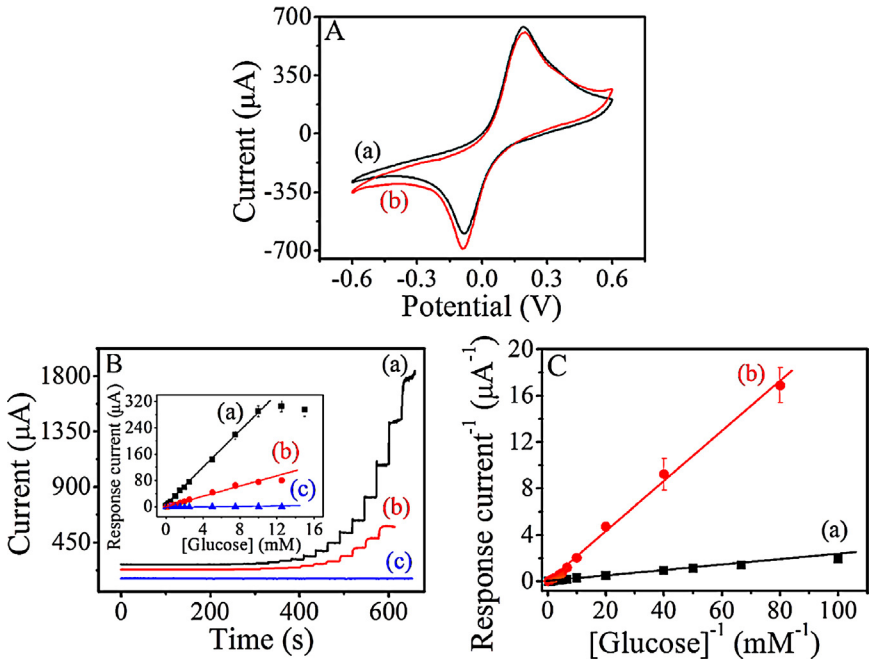

Fig. 6. (A) CVs of the GOD-PBBIns-Gs/Au electrode in the (a) absence and (b) presence of 5 mM glucose. (B) Current–time plots of the (a) GOD-PBBIns-Gs/Au, (b) GOD-PBBIns/Au, and (c) PBBIns-Gs/Au electrodes after the successive addition of glucose at increasing concentrations. Inset: The linear dependence of response currents vs. glucose concentrations ($n = 5$). (C) Lineweaver–Burk plots for the (a) GOD-PBBIns-Gs/Au and (b) GOD-PBBIns/Au electrodes.

response time as well as high biological affinity, most likely because of its high sensitivity toward released H_2O_2, superior loading of GOD, and favorable bioactivity. Additionally, it has been reported that GOD maintains optimal bioactivity at pH 6.0, which is similar to the value of pH 6.4 used in this study [48].

3.6. Reproducibility and selectivity of the glucose biosensor

The reproducibility of the glucose biosensor was investigated by measuring 1 mM glucose five times; the relative standard deviation (RSD) was 4.5%, which indicates that the biosensor measurements are reproducible. As expected, neither ascorbic acid (AA, 1 mM) nor uric acid (UA, 1 mM) interfered with the response current for 1 mM glucose. Moreover, the response current did not change in the presence of bovine serum albumin (BSA, 100 nM), which indicates that the biosensor is highly selective (Fig. 7A). Furthermore, the thermal stability of the H_2O_2 PBBI/Au sensor-based electrode was excellent in previous reports [35]. The main factor that influenced the stability of the glucose biosensor was GOD bioactivity. To investigate long-term stability, the GOD-PBBIns-Gs/Au electrode with 20 U of GOD was stored at 4 °C in PBS for 10 days. The electrode retained approximately 92.3% of bioactivity relative to the initial electrode (Fig. 7B). This result demonstrates that the glucose biosensor maintained stability, most likely because the nanostructures of PBBIns and Gs provided a suitable nano-environment for GOD.

3.7. Potential application in a choline biosensor

To further illustrate the advantages of the PBBIns-Gs/Au electrode in oxidase-based amperometric biosensors, a similar procedure was employed for choline detection, where H_2O_2 was produced during the choline–choline oxidase (ChOx) reaction.

$$\text{Choline} + O_2 \xrightarrow{\text{ChOx}} \text{betaine aldehyde} + H_2O_2$$

In contrast to GOD-PBBIns-Gs/Au electrode preparation, in which GOD-PBBIns-Gs was prepared prior to addition to the Au electrode, the PBBIns-Gs/Au electrode was constructed and then dipped into a ChOx solution for 30 min for adsorption of ChOx. After the free enzyme was washed off, the ChOx-PBBIns-Gs/Au electrode was used for choline determination. Fig. 8A illustrates the chronoamperometric response of the ChOx-PBBIns-Gs/Au electrode to various choline concentrations at pH 6.4. Under an applied potential of −0.5 V and in an unstirred system, the reduction current increased with time and stabilized with an increase in choline concentration in which the current did not response without ChOx. Fig. 8B depicts the calibration curve of the current response to choline concentration based on the probe of the ChOx-PBBIns-Gs/Au electrode. This electrode exhibited a linear range from 0.1 μM to 0.83 mM with a sensitivity of 494.9 μA mM^{-1} cm^{-2}. The detection limit was estimated to be 0.02 μM ($S\,N^{-1} = 3$). These data indicate that the development of a choline biosensor is feasible through immobilization ChOx on the PBBIns-Gs/Au electrode.

Table 1
Analytical properties of different glucose biosensors.

	Sensitivity (μA mM^{-1} cm^{-2})	Linear range (mM)	Response time (s)	K_m^{app} (mM)	Ref.
GOD/PdNPs/CS-GR	–	0.001–1.0	10.0	1.2	[49]
Au-PANI-(CS-CNTs)-GOD	–	1.0–20.0	8.0	5.35	[50]
pCoTTP-SWNTs-Nafion-GOD	16.57	Up to 1	15.0	0.98	[51]
PTMSPA/HRP-GOx	5.1	1.0–20.0	7.0	5.76	[52]
GOD-PBBIns/Au	40.6	0.0125–7.5	6.9	1.24	This study
GOD-PBBIns-Gs/Au	143.5	0.01–10.0	5.6	0.54	This study

(–) Data not available.

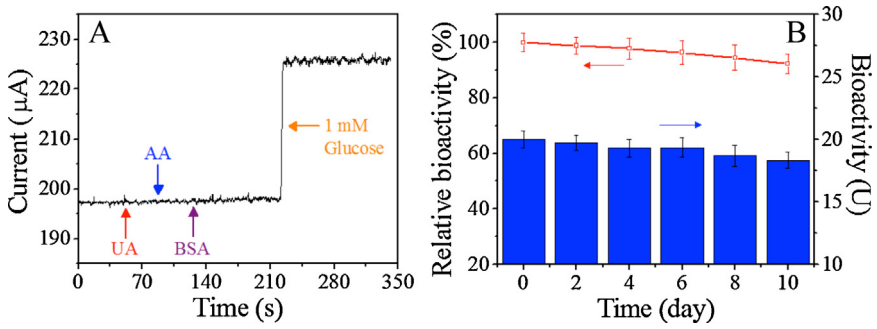

Fig. 7. (A) Effects of interfering species on the response currents of the GOD-PBBIns-Gs/Au electrode in 1 mM glucose. (B) Stability and bioactivity of the GOD-PBBIns-Gs/Au electrode stored at 4 °C in PBS over time.

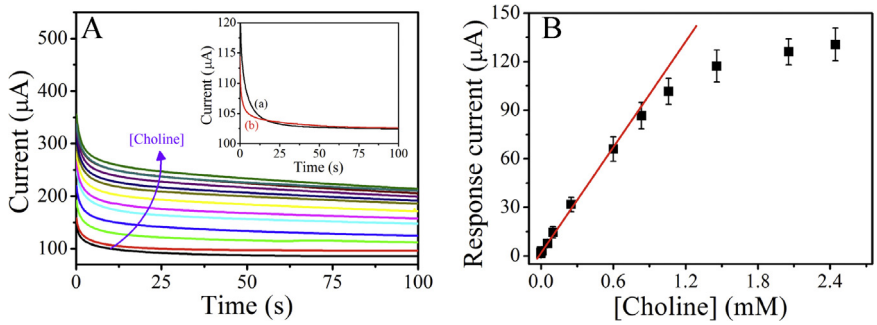

Fig. 8. (A) Current–time plots of the ChOx-PBBIns-Gs/Au electrode in the presence of 0, 1, 6, 10, 50, 100, 250, 600, 830, 1060, 1460, 2056, and 2445 μM choline. Inset: Current–time plots of the PBBIns-Gs/Au electrode without and with 830 μM choline. (B) Linear dependence of response currents on choline concentration based on ChOx-PBBIns-Gs/Au electrode ($n = 5$).

4. Conclusions

A colloidal suspension of PBBIns-Gs was used for oxidase loading in the development of a biosensor based on the release of H_2O_2. The intercalation between Gs and acid-treated PBBIns separated PBBIns and Gs simultaneously, which generated numerous channels and pores for H_2O_2 diffusion and resulted in enhanced performance of the H_2O_2 sensor relative to the sensor in the absence of Gs. In addition, positively charged PBBIns not only made the colloidal composite disperse well in DI water, which is a suitable environment for the enzyme, but also attracted the negative charge of GOD or ChOx directly via electrostatic interactions. Moreover, the non-destructive immobilization preserved high enzyme bioactivity. These advantages provide a favorable platform for the development of oxidase-based biosensors.

Acknowledgements

We thank the National Science Council of the Republic of China, Chang Gung University, and the Industrial Technology Research Institute for financial support: CMRPD2A006(1-2), UERPD2B0281, NSC 101-3113-E-182-011-CC2, NSC 101-2221-E-182-011-MY3, NSC 100-2221-E-182-005, and CF51RQ3000.

References

[1] A.P. Turner, B. Chen, S. Piletsky, Clin. Chem. 45 (1999) 1596–1601.
[2] A.I. Gopalan, K.P. Lee, D. Ragupathy, D.S.H. Lee, J.W. Lee, Biomaterials 30 (2009) 5999–6005.
[3] J.D. Qiu, R. Wang, R.P. Liang, X.H. Xia, Biosens. Bioelectron. 24 (2009) 2920–2925.
[4] K.M. Manesh, H.T. Kim, P. Santhosh, A.I. Gopalan, K.P. Lee, Biosens. Bioelectron. 23 (2008) 771–779.
[5] M. Yang, J. Jiang, Y. Lu, Y. He, G. Shen, R. Yu, Biomaterials 28 (2007) 3408–3417.
[6] H.W. Yang, M.Y. Hua, S.L. Chen, R.Y. Tsai, Biosens. Bioelectron. 41 (2013) 172–179.
[7] H. Qiu, L. Xue, G. Ji, G. Zhou, X. Huang, Y. Qu, P. Gao, Biosens. Bioelectron. 24 (2009) 3014–3018.
[8] M. Chen, W. Zhang, R. Jiang, G. Diao, Anal. Chim. Acta 687 (2011) 177–183.
[9] S. Chakraborty, C.R. Raj, Biosens. Bioelectron. 24 (2009) 3264–3268.
[10] S. Thiagarajan, S.M. Chen, Talanta 74 (2007) 212–222.
[11] Y.Q. Dai, D.M. Zhou, K.K. Shiu, Electrochim. Acta 52 (2006) 297–303.
[12] M. Cano, J.L. Ávila, M. Mayén, M.L. Mena, J. Pingarrón, R. Rodríguez-Amaro, J. Electroanal. Chem. 615 (2008) 69–74.
[13] J. Lu, L.T. Drzal, R.M. Worden, I. Lee, Chem. Mater. 19 (2007) 6240–6246.
[14] F. Qu, A. Shi, M. Yang, J. Jiang, G. Shen, R. Yu, Anal. Chim. Acta 605 (2007) 28–33.
[15] O. Nadzhafova, M. Etienne, A. Walcarius, Electrochem. Commun. 9 (2007) 1189–1195.
[16] V. Vojinović, F.M.F. Esteves, J.M.S. Cabral, L.P. Fonseca, Anal. Chim. Acta 565 (2006) 240–249.
[17] V. Vojinović, C.R. Calado, A.I. Silva, M. Mateus, J.M.S. Cabral, L.P. Fonseca, Biosens. Bioelectron. 20 (2005) 1955–1961.
[18] M.A. Rahman, M.S. Won, Y.B. Shim, Biosens. Bioelectron. 21 (2005) 257–265.
[19] J.G. Franchina, W.M. Lackowski, D.L. Dermody, R.M. Crooks, D.E. Bergbreiter, K. Sirkar, R.J. Russell, V.M. Pishko, Anal. Chem. 71 (1999) 3133–3139.
[20] Y. Astuti, E. Topoglidis, A.G. Cass, J.R. Durrant, Anal. Chim. Acta 648 (2009) 2–6.
[21] A. Ahmadalinezhad, A.K.M. Kafi, A. Chen, Electrochem. Commun. 11 (2009) 2048–2051.
[22] F. Palmisano, R. Rizzi, D. Centonze, P.G. Zambonin, Biosens. Bioelectron. 15 (2000) 531–539.
[23] A. Mignani, E. Scavetta, D. Tonelli, Anal. Chim. Acta 577 (2006) 98–106.
[24] J. Wang, X.J. Zhang, Anal. Chem. 73 (2001) 844–847.
[25] J. Kulys, L. Tetianec, P. Schneider, Biosens. Bioelectron. 16 (2001) 319–324.
[26] X.B. Yan, X.J. Chen, B.K. Tay, K.A. Khor, Electrochem. Commun. 9 (2007) 1269–1275.
[27] N. Ferreyra, L. Coche-Guérente, P. Labbé, Electrochim. Acta 49 (2004) 477–484.
[28] J. Zhang, M. Feng, H. Tachikawa, Biosens. Bioelectron. 22 (2007) 3036–3041.
[29] Y. Liu, D. Yu, C. Zeng, Z. Miao, L. Dai, Langmuir 26 (2010) 6158–6160.
[30] O.M. Schuvailo, O.O. Soldatkin, A. Lefebvre, R. Cespuglio, A.P. Soldatkin, Anal. Chim. Acta 28 (2006) 573–574.
[31] D. Wen, Y. Liu, G.C. Yang, S.J. Dong, Electrochim. Acta 52 (2007) 5312–5317.
[32] Y. Wang, X. Wang, B. Wu, Z. Zhao, F. Yin, S. Li, X. Qin, Q. Chen, Sens. Actuat. B 130 (2008) 809–815.
[33] H. Yang, Y. Zhu, D. Chen, C. Li, S. Chen, Z. Ge, Biosens. Bioelectron. 26 (2010) 295–298.
[34] Y. Tan, W. Deng, C. Chen, Q. Xie, L. Lei, Y. Li, Z. Fang, M. Ma, J. Chen, S. Yao, Biosens. Bioelectron. 25 (2010) 2644–2650.
[35] M.Y. Hua, H.C. Chen, R.Y. Tsai, Y.C. Lin, L. Wang, Anal. Chim. Acta 693 (2011) 114–120.
[36] M.Y. Hua, H.C. Chen, R.Y. Tsai, Y.L. Leu, Y.C. Liu, J.T. Lai, J. Mater. Chem. 21 (2011) 7254–7262.

[37] J. Han, H. Kim, D.Y. Kim, S.M. Jo, S.Y. Jang, ACS Nano 4 (2010) 3503–3509.
[38] J. Yan, T. Wei, B. Shao, Z. Fan, W. Qian, M. Zhang, F. Wei, Carbon 48 (2010) 487–493.
[39] M.Y. Hua, H.C. Chen, R.Y. Tsai, Y.C. Lin, Electrochim. Acta 56 (2011) 4618–4623.
[40] M.Y. Hua, H.C. Chen, C.K. Chuang, R.Y. Tsai, J.L. Jeng, H.W. Yang, Y.T. Chern, Biomaterials 32 (2011) 4885–4895.
[41] Y. Zhang, X. Sun, L. Zhu, H. Shen, N. Jia, Electrochim. Acta 56 (2011) 1239–1245.
[42] M. Yang, J. Jiang, Y. Lu, Y. He, G. Shen, R.R. Yu, Biomaterials 28 (2007) 3408–3417.
[43] E. Laviron, J. Electroanal. Chem. 52 (1974) 355–393.
[44] E. Laviron, J. Electroanal. Chem. 100 (1979) 263–270.
[45] Y. Su, W. Huang, R. Hu, H. Ding, K. Hu, Biosens. Bioelectron. 24 (2009) 2665–2670.
[46] R.A. Kamin, G.S. Wilson, Anal. Chem. 52 (1980) 1198–1205.
[47] H. Wang, X. Wang, X. Zhang, X. Qin, Z. Zhao, Z. Miao, N. Huang, Q. Chen, Biosens. Bioelectron. 25 (2009) 142–146.
[48] X. Han, Y. Zhu, X. Yang, J. Solid State Electrochem. 15 (2011) 511–517.
[49] Q. Zeng, J.S. Cheng, X.F. Liu, H.T. Bai, J.H. Jiang, Biosens. Bioelectron. 26 (2011) 3456–3463.
[50] D. Wan, S. Yuan, G.L. Li, K.G. Neoh, E.T. Kang, ACS Appl. Mater. Interfaces 2 (2010) 3083–3091.
[51] W. Chen, Y. Ding, J. Akhigbe, C. Bruckner, C.M. Li, Y. Lei, Biosens. Bioelectron. 26 (2010) 504–510.
[52] K.M. Manesh, P. Santhosh, S. Uthayakumar, A.I. Gopalan, K.P. Lee, Biosens. Bioelectron. 25 (2010) 1579–1586.